JJMIE

Volume 18, Number 1, March. 2024
ISSN 1995-6665
Pages 99- 112
https://doi.org/10.59038/jjmie/180108
Editor-in-Chief: Prof. Ali M. Jawarneh

Jordan Journal of Mechanical and Industrial Engineering

Synergistic Enhancement of Sunflower Lubricant Incorporated Anti-Wear Eichhornia Crassipes and Tertiary-Butyl-Hydroquinone (TBHQ) Additives

Anthony Chukwunonso Opia[1,2,3], MohdFadzli Bin Abdollah[1,2*], Hilmi Amiruddin[1,2], Mohd Kameil Abdul Hamid[4], IbhamVeza[5], Fazila Binti Mohd Zawawi[4]

[1]*Faculty of Mechanical TEchnology and Engineering, Universiti Teknikal Malaysia Melaka, Hang Tuah Jaya, 76100 Durian Tunggal, Melaka, Malaysia.*
[2]*Centre for Advanced Research on Energy, UniversitiTeknikal Malaysia Melaka, Hang Tuah Jaya, 76100 Durian Tunggal, Melaka, Malaysia.*
[3]*Department of Marine Engineering, Niger Delta University, Wilberforce Island Amassoma, PMB 071, Bayelsa, Nigeria*
[4]*Automotive Development Centre, School of Mechanical Engineering, UniversitiTeknologi Malaysia, Johor Bahru 81310, Malaysia.*
[5]*Department of Mechanical Engineering, UniversitiTeknologi PETRONAS, 32610 Seri Iskandar, Perak, Malaysia*

Received 31 Aug 2023 *Accepted 3 Dec 2023*

Abstract

Due to the impending depletion of petroleum reserves and environmental worries, the creation of bio-lubricants is a compelling subject of research. With the use of tertiary butylhydroquinone (TBHQ) and Eichhornia crassipes carbon nanotubes (EC-CNTs), this work intends to create an effective sunflower oil-based bio-lubricant and analyze its tribological performance using a ball-on-disk tribo-meter. Different additive concentrations were blended to create the bio-lubricant. The tribological analysis was conducted in terms of coefficient of friction (COF), wear rate, wear scar diameter, surface roughness for different speed, load and temperature. The morphology shows good structures of the employed additives, TGA revealed good thermal resistance, FT-IR indicated good compatibility with needed functional groups. Under tribological test at 1500 rpm, inclusion of additives (SFO + 0.9wt.% EC-CNTs + 0.3wt.% TBHQ) demonstrated good enhancement on sunflower lubrication, thus showing COF and wear rate values of 0.058 and 13.5 10^{-9} $mm^3.m^{-1}.N^{-1}$ against base sunflower COF and wear rate values of 0.074 and 15.5 $*10^{-9}$ $mm^3.m^{-1}.N^{-1}$. Under surface roughness, application of additives lowers the roughness on the lubricated surfaces (SFO + 0.9 wt.% EC-CNTs = 0.447 µm), (SFO + 0.3 wt.% TBHQ = 0.453 µm), thus shows smoothest when blended the two additives together (SFO + 0.9 wt.% EC-CNTs + 0.3 wt.% TBHQ = 0.244 µm), against base SFO value of 0.522 µm. The use of additives in SFO shows synergistic result via nano-lubricant tribo-film formation resulting in commended outcome in all the conditions tested.

Keywords: Vegetable lubricant; TBHQ and EC-CNTs additives; lubrication, friction and wear.

1. Introduction

The preservation of resources and energy is increasingly becoming a major worldwide issue as to maintain a sustainable society, foster industrialization, development and effective production. In industrial processing, mostly for mechanical system, friction is the principal source of energy loss [1], that lubrication can help to mitigate [2][3][4]. For optimal lubrication, it is important to use the right base oil and suitable additives [5][6][7], as there is an increased interest in environmental issues around the world resulting on formulating a suitable eco-friendly lubricant in replacing petroleum products that are associated with some toxic constituents [8][5][9]. As a result, research into creating and patronizing vegetable oils as substitute base-oils for lubricants that are eco-friendly has increased [10][11]. In addition to being made from renewable raw materials, vegetable oils are also biodegradable and non-toxic, making them possible replacements for petroleum products [12][11][13]. Additionally, they possess majority of lubricant-specific qualities, including a high viscosity index, low volatility, excellent lubricity, and a remarkable potential to dissolve fluid additives [14][5][15].

Regarding oil content, sunflower oil is one of the most significant vegetable oils, and it also ranks highly in terms of relevance for human nutrition [16]. In terms of fatty acid profiles, sunflower seeds and oils have significantly improved [16]. Within the last 20 years, plant breeders and geneticists have successfully commercialized mid- and high-oleic varieties to address the stability issue. Due to

* Corresponding author e-mail: mohdfadzli@utem.edu.my.

the high content of oleic acid relative to other vegetable oils, modified sunflower oils have been demonstrated to have outstanding oxidative stability in both high-temperature applications and where foods need a long shelf life [16][17][18]. Additionally, sunflower has favorable tribological properties and a fatty acid content that is predominately polyunsaturated [17]. Sunflower oil's various fatty acid compositions improve its tribological characteristics by reducing wear and friction. However, due to the unsaturation nature of sunflower oil, made up of less stable monounsaturated and polyunsaturated fatty acids, heat and air can rapidly degrade it, accelerating its oxidation.

In addressing the challenge, inclusion of suitable lubricant additives can be used to enhance the thermal characteristics of sunflower oil [19], or via chemical modifications like epoxidation, transesterification, or selective hydrogenation [20][21][22]. Liu et al., [23], conducted tribological enhancement of base lubricant performance and thermal losses of palm oil (PO) using tertiary butylhydroquinone (TBHQ) as an additive. The results revealed that TBHQ had better antioxidant activities at low temperatures (below 135°C), but at high temperatures (above 135°C), its antioxidative resistance to PO was severely reduced. The reported results were similar with Ali et al., [24]. Additionally, losses of TBHQ in PO substantially increased when heating temperatures rose, and heating periods lengthened.

Numerous studies on the use of nanoparticles (NPs) in the field of lubrication have been conducted recently [25][26][27]. The size, shape, and concentration of NPs all affect how much friction and wear may be reduced. According to recent studies [28][29][30], an important factor in the formulation of nano-lubricants is the concentration of nanoparticles in the base oils. Ettefaghi et al., [29][31], affirmed that base oils can be upgraded to have the required quality with only a little concentration of nanoparticles. More so, research has confirmed that load, speed, temperature, and concentration are often the main considerations when assessing the tribological characteristics of nano-lubricants [32][28]. Therefore, in this study, the effectiveness of a sunflower (SFO) lubricant combined with an Eichhornia crassipes carbon nanotubes (EC-CNTs) anti-wear additive and an antioxidant agent (TBHQ) will be assessed and analyzed in terms of coefficient of friction, wear scar rate, surface roughness, and the wear scar diameter. The use of EC-CNTs in the study was based on the performance seen in the prior investigations [27], thus necessary to determine their synergetic enhancement with TBHQ during lubrication.

1.1. Sunflower oil nature and its molecular structure

Sunflower oil is a non-volatile oil that is extracted from the sunflower plant's seeds. It is frequently used as frying oil in food and as an emollient in cosmetic applications. It is mostly composed of oils from the Oleic Acid ($CH_3(CH_2)_7CH=CH(CH_2)_7COOH$) (Omega-9 fatty acid) and Linoleic Acid ($COOH(CH_2)_7CH=CHCH_2CH=CH(CH_2)_4CH_3$) (Omega-6 fatty acid) groups [33][34][35][36], which are both monounsaturated and polyunsaturated as presented in Figure 1. The unsaturated double bonds in the fatty acid chain ruin the oil's characteristics. These very unstable unsaturated double bonds lead to chemical processes, such as the oxidation process. Analyzing SFO compositions, the kernel contains 45–55% oil, while the seed's oil content ranges from 22% to 36% (on average 28%) [34]. The refined oil is pale yellow, whereas the expressed oil is light amber in color and flavor. Significant amounts of vitamin E, sterols ($C_{17}H_{28}O$), squalene ($(C_5H_8)_6$), and other aliphatic hydrocarbons are present in refined sunflower oil [34].

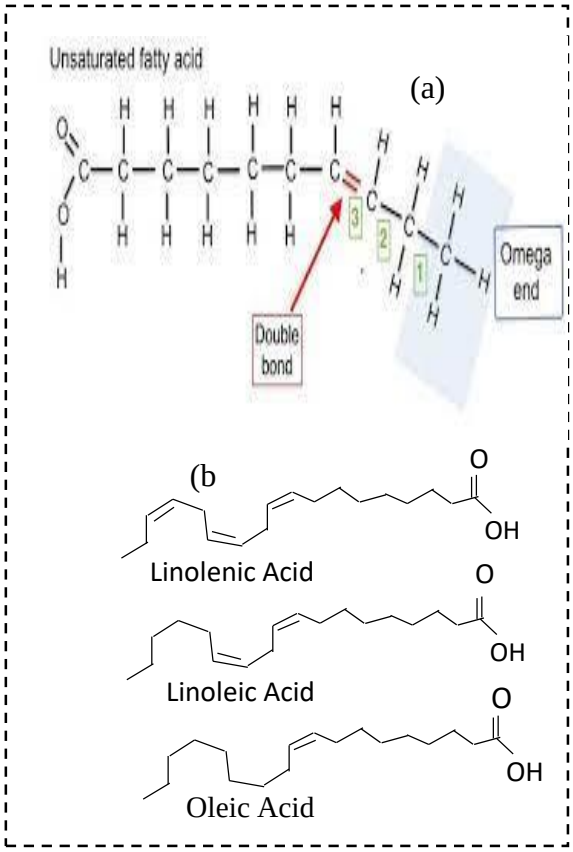

Figure 1. Images showing the sunflower double bond (a); linolenic acid (omega-3), linoleic acid (omega-6), oleic acid (omega-9) (b).

2. Materials and experimental procedure

2.1. Base-oil and additives selected

Using tribometers, variations in the characteristics of sunflower generated in pure state and by inclusion of EC-CNTs and TBHQ nanoparticles on a weight % basis will be investigated in this research. Sunflower oil lubricants is chosen in this investigation because, in the boundary lubrication regime, vegetable oils typically exhibit good lubricating capabilities [37], expected more enhancement under anti-wear and anti-oxidant additives. The TBHQ ingredient was purchased from Sigma-Aldrich Co. LLC in Malaysia together with sunflower oil, while bearing and disc were purchased from Atlas Ball and Bearing Co. Ltd. Malaysia. In the material laboratory of UniversitiTeknologi Malaysia, the organic anti-wear EC-CNTs was formulated.

2.2. Formulation of nano-lubricants

The TBHQ and EC-CNTs NPs were combined with pure sunflower lubricant at varying concentrations. Base-oilof 500 mL without any additive was used for making each nano-lubricant. The EC-CNTs nanoparticles were added to the oil on weight percentage basis, such as 0.3, 0.6, 0.9 and 1.1wt.%, while TBHQ of 0.3 wt.% was maintained. The choice of using 0.3wt.% of TBHQ was due to the previous study conducted, suggesting little concentration [24]. To ensure uniform dispersion and good suspension stability, the solution was then stirred using an ultrasonic mixer for 50 min under 2500 rpm. This was done in order to reduce the van der Waals force of attraction between the particles and control their aggregation in solution.

2.3. Characterization of the samples

In this study, the morphology and nano-size of the chosen additive were examined. Field emission scanning electron microscope (FESEM) (HITACHI SU6600) incorporated with Energy dispersive spectroscopy (EDS) (HORIBA- EMAX) were used to characterize EC-CNTs and TBHQ. For oxidation resistance of the TBHQ in SFO, using 5 mg samples enclosed in hermetically sealed aluminum pans, differential scanning calorimetry (DSC) study were carried out with a Q–100 TA equipment. All samples were subjected to cooling and heating rates of 10 C/min, which is ideal with advantages of being quick and having more repeatable results [38]. The temperature window chosen covered a flow rate of 50 mL/min between 150 and 400 °C. In order to identify the functional groups and determine if oil lubricant and specially designed EC-CNT could coexist, Fourier-transform infrared spectroscopy (FT-IR) investigation was carried out. To determine the nature of the anti-wear additive (EC-CNT) and physio-chemical characteristics of the selected additives, thermal strength tests were performed on the samples of EC-CNTs, TBHQ and EC-CNT + TBHQ blends with oil using Raman spectroscopy and thermogravimetric analysis (TGA) analysis, respectively.

2.4. Rheological studies

When describing a lubricant for industrial use, assessments of the rheological characteristics of the formulations are significant. Kinematic viscosity at various temperatures is the main rheological parameter that is examined in this work. A Redwood Viscometer that meets ASTM D-445 requirements is used to gauge the viscosity of base lubricant and nano-formulations. Each trial uses 125 mL of oil, thus generated by the system via excel. The viscosity index of the kinematic viscosity from the viscometer were determined using viscosity index system calculator. Each sample undergoes three trials. At temperature range of 30-150 °C, the fluctuations in kinematic viscosity were measured.

2.5. Tribological study

As shown in Figure 2, a Wind-Ducom instrument 2010 (USA) ball-on-disc tribometer is used to conduct the tribological examinations of the base-oils and nano-lubricants. The ASTM G 99-05 guidelines were followed when conducting tribological studies. By installing an appropriate accessory for heating the oil delivered to the traditional ball-on-disc tribometer, it was possible to measure the differences in the tribological properties of the lubricants at higher temperatures. The heating connection is made up of a temperature sensor, lubricant holder, and heating coil. The disc is made of steel (EN-GJL 250) with a hardness of 60 HRC, and the ball material is made up of steel AISI 52100 steel (0.98-1.1% C, 1.30-1.60 % Cr, 0.25-0.45% Mn, 0.025% P, 0.025% S, 0.15-0.30% Si,). The ball and disc diameters were 8 mm and 80 mm, respectively.

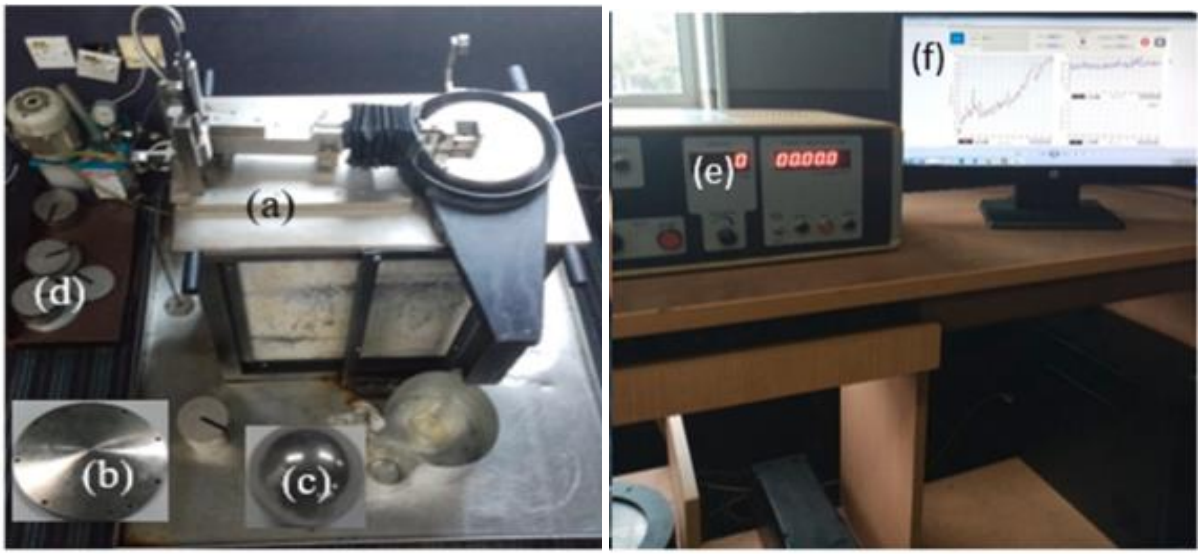

Figure 2. Image of ball on disc set up (unidirectional mode); (a), ball on disc machine; (b), disc; (c), ball; (d), loads; (e), system panel; (f), system monitor.

The sliding surface of the steel ball was at finished polished, similar polishing conditions were used for the steel disc. To avoid contamination during preparation, acetone was used to clean the surfaces. According to measurements from a profilometer, the roughness value (Ra) on a ball's surface ranges from 0.025 to 0.050 µm, and disk's surface, was between 0.2 and 0.5 µm. The disc slides at speeds, normal load as stated in Table 1.

To maintain boundary/thin film lubrication conditions, oil is delivered at the sliding interface between the steel ball and steel disc on the Wind-Docom ball-on-disc tribometer in small amounts (drop-wise approach). Utilizing a load cell, an electronic display, and the thickness of the lubricant film, frictional force is directly measured. The ball is weighed before and after sliding on an electronic weighing balance with a minimum count of 0.1 mg, and the wear rater is then calculated. Each testing sample undergoes three trials in order to ensure the results are reproducible. The performance variables COF and specific wear rate were assessed based on the average results of three trial tests that were run for each input parameter.

Table 1. Test conditions for the pin-on-disc analysis

Parameter	Value
Load (N) (variable parameters)	60, 80, 100, 120
Temperature (ºC) (variable parameter)	55, 75, 100
Speed (rpm)	1100, 1300, 1500, 1700
Test duration	1 hr
Contact pressure	798 MPa
Disc (lower test piece)	EN-GJL-250, Dia. 165 mm
Ball (upper test piece)	AISI52100, Dia. 10 mm

2.6. Wear scar diameter and surface topography analyses

The wear scar diameter (WSD) of the lubricated surfaces was measured using FESEM, with magnification ranges from 150 to 180 for the ball's friction surface, while the surface roughness (Ra) was measured using a surface profilo-meter in order to examine the

surface topography. The disc volume loss was calculated using Equation 1.

However, the linear speed remains constant throughout the testing because the sliding speed is translated to RPM suitably for each sliding radius of the disc. The wear specific rate or wear rate been the amount of material loss under a particular sliding distance, thus calculated using Equation (2). Sliding distance = Sliding speed × Test duration time

$$Disvolumeloss, mm^3 = \frac{\pi(weartrackradius,mm)(weartrackdiameter,mm)^3}{5\,(ballradius,mm)} \quad (1)$$

$$Wear\ Specific\ rate = \frac{Wear\ Volume,\ m^3}{Sliding\ Distance,\ m} \quad (2)$$

3. Results and Discussions

3.1. Characterization and rheological study

Figure 3 depicts FESEM illustrations of the surface morphology of the newly formulated EC-CNTs anti-wear and TBHQ antioxidant additives. Figure 5 (a) shows a high resolution of EC-CNTs with a tube-like structure, while TBHQ exhibited a gel skeletal like structure. This result implies that the additives were effectively prepared. The EDS displays the elements found in the samples mentioned in Table 2, obtained from the FESEM images. The information obtained in the previous research [39] was similar to the elements found in this presented study.

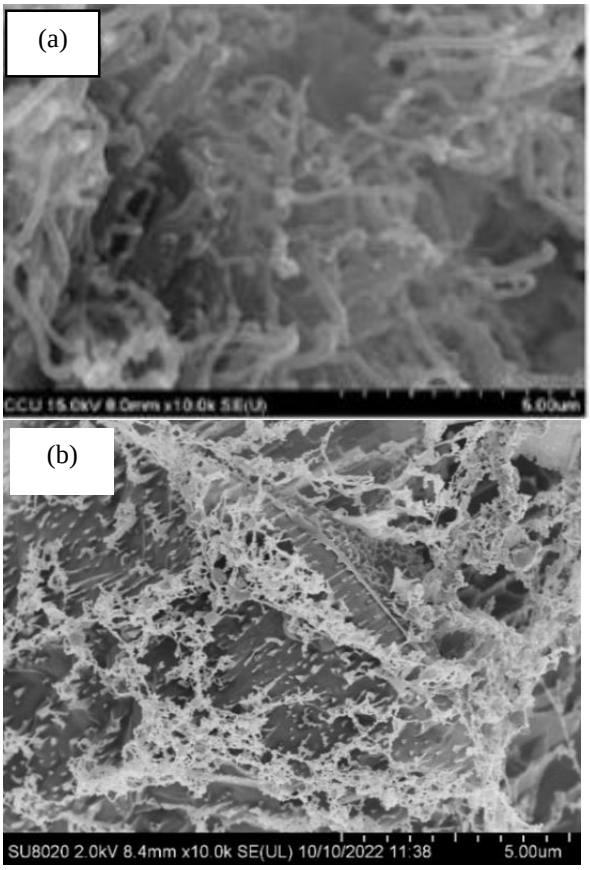

Figure 3. FESEM images of EC-CNT anti-wear (a) and TBHQ antioxidant additive (b) used.

Table 2. EDX elemental composition in TBHQ and EC-CNTs additives used.

Sample/Element (wt.%)	C	O	K	Fe	Mg	Al	Si	Cl	S	Mn	Na	Ca	P
TBHQ	79.7	20	-	-	-	-	-	-	-	-	-	-	-
EC-CNTs	64.3	17.4	5.4	0.4	0.9	0.4	3.7	3.6	0.4	1.4	0.2	1.3	0.2

Using a dynamic light scattering (DLS) particle size machine, Figure 4 displays the particle size distribution. The TBHQ shows an average particle size of 18.8 nm, meeting the requirements set for industrial application. The data show that polar and non-polar N-Methyl-2-pyrrolidone solutions, with average mean diameters of 58.3 nm, for dispersing EC-CNTs. The TBHQ has a bulk density of 0.67 103 kg/m^3 and a metallic brown shape that is generally spherical.

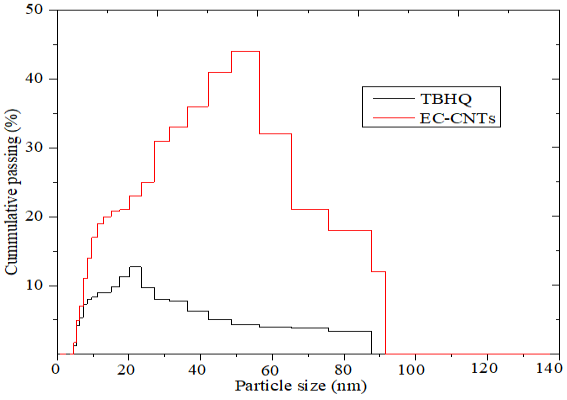

Figure 4. Particle size distributions of TBHQ and EC-CNTs additives

Figure 5. depicts the result of Oxidation analysis of SFO only and SFO + TBHQ tested (a) and FT-IR spectra of the various lubricants The antioxidant activity of the TBHQ additive was investigated in detail on its degradation resistance as presented in Figure 5 (a). TBHQ's concentration of 0.3 wt.% was used to determine its antioxidant capability sunflower base oil. The concentration used was chosen based on previous study [24]. The concentration of TBHQ added in the base oil was 0.3 wt.%. DSC was used to determine the initial oxidation temperature (IOT) and oxidation induction time (OIT). Better oxidation stability of the sample is indicated by a greater IOT and longer OIT. When TBHQ was added, the IOT value was 289 ºC, compared to base SFO oil, which had only 237 ºC. The introduction of an antioxidant agent, which significantly increases the antioxidant potency, as indicated by the significantly higher IOT values of the TBHQ addition compared to base SFO. Additionally, when the end points of the samples were compared, it was clear that the base SFO vanished at 328 ºC, while the addition of TBHQ resulted in elimination at 367 ºC, simply demonstrating the antioxidant ability. This indicates that the molecular weights of the compounds in TBHQ are well compatible with the SFO lubricant, leading to excellent performance.

As depicted in Figure 5(b), the functional group CH_2 inside a long fatty alkyl chain displayed symmetric vibration at 2880 cm^{-1} and antisymmetric stretching vibration peak at 2725 cm^{-1} for all the samples but more pronounced with the SFO + TBHQ +EC-CNTs. Given that the absorption peaks formed at the wave numbers of 1842 cm^{-1} and 1781 cm^{-1}, and that the smaller wave number peak was stronger than the larger wave number peak, can infer that EC-CNT and TBHQ were found in the mixture of SFO + TBHQ + EC-CNTs. The vibration shift on COO- groups seen in base SFO and SFO + TBHQ + EC-CNTs with asymmetric and symmetric stretching is responsible for the discovery of two additional peaks at 1602 and 1632 cm^{-1}, which are shorter than formation observed in TBHQ and EC-CNTs separately, indicating good binding in the presence of SFO.

Additionally, a notable shift in the SFO + TBHQ + EC-CNTs sample was seen at 1583 cm^{-1} due to the poor COO- group concentration, and the N-H bond of the organic complex which brings the absorption peak of SFO and SFO + TBHQ + ECNTs so close at 1250 cm^{-1}. The long peak (SFO + TBHQ + ECNTs) at 1170 cm^{-1} was the result of aromatic C-H out of plane bends, whereas band 1017 cm^{-1} was the result of hidden C-O-C stretch behavior due to -OH bending of cellulose, lignin, and hemicellulose constituents present in EC-CNTs. As a result of ester cleavage and the production of a carboxyl group in EC-CNTs, changed and shifted to a new value about 1695 cm^{-1} when blended with SFO and TBHQ. In conclusion, the same graph train among the SFO and SFO +TBHQ + EC-CNTs demonstrates compatibility between the additives and the base oil, and is commended. Additionally, it was found that the functional groups seen in the formulations' FT-IR analysis were essential in strengthening the tribological characteristics of the lubricant.

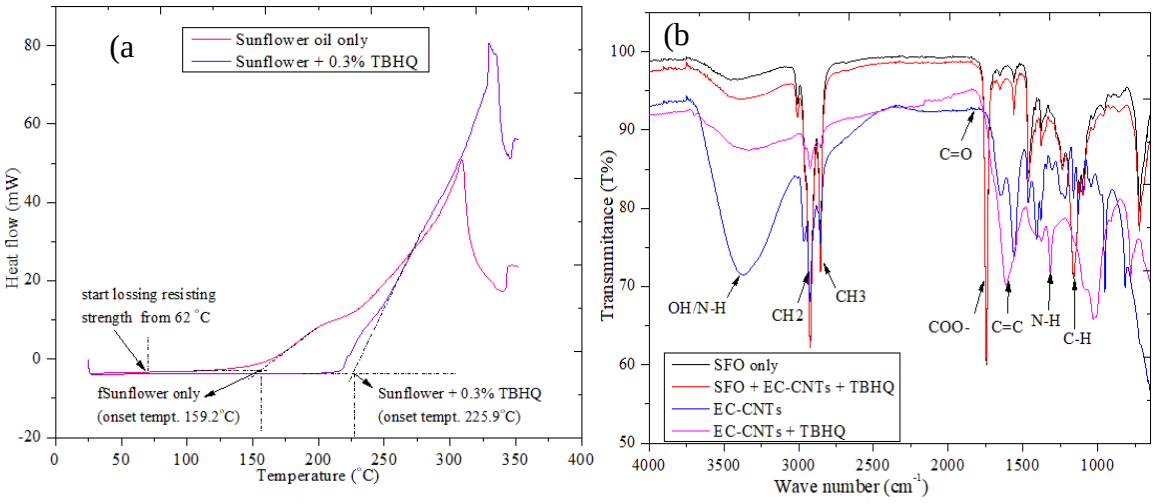

Figure 5. Oxidation analysis of SFO only and SFO + TBHQ tested (a) and FT-IR spectra study of SFO, EC-CNTs + TBHQ, EC-CNTs, and SFO + TBHQ + EC-CNTs tested (b).

Figure 6 display images of the TGA and Raman spectroscopy studied, respectively. Fig. 6(a) shows the TGA results of SFO, SFO + TBHQ, SFO + EC-CNTs, and SFO + TBHQ + EC-CNTs, respectively. The weight loss percentage was determined using derivative thermos-gravimetric data [40]. Before the inclination caused by degradation from the various lubricant samples, at the intersection of two tangents derived from a thermos-gravimetric curve, the onset degradation temperature was discovered. SFO weight loss was 38.5%, which may be attributed to contaminants or features of contents possible of fasting degradation. After being modified with EC-CNT, the weight loss was 18%, according to Fig. 6(a), modifications with TBHQ yielded weight loss of 14.7%, showing good heat resistance from antioxidant additive.

The lubricant blended with TBHQ + EC-CNTs shows synergistic enhancement with 13.3% weight loss. The changes suggest that the thermal properties of SFO have been improved due to thermal degradation resistance from TBHQ + EC-CNTs. Compared to SFO, the weight loss of TBHQ and EC-CNTs were significantly lower, which may be attributed to the constituents and the formulations procedure, leading to improved thermal properties. The Raman spectroscopy study was presented in Figure 6 (b). The results show two distinct peaks in the D-band and G-band at 1375.31 and 1601.37 cm^{-1}, respectively, caused by carbon atom vibrations in the graphene layer. The treatments led to the accessibility of sp^3 carbon hybridization [41]. These results are similar to those obtained by Nasir et al.,[42] to investigate carbon nanotubes. The prepared sample of EC-CNTs in this analysis, revealed that D-band is less than G-band (ID < IG), as shown in Figure 6(b), indicated that the G-band peak is greater than the D-band, thus proves the product carbon nanotubes.

Figure 7 shows the viscometric properties of SFO alone as well as the addition of the EC-CNT (0.3, 0.6, 0.9, and 1.1 wt. %) and TBHQ (0.3 wt.%) additives that were examined in this work. The test used centistoke viscosity at temperatures between 40 and 150 °C and specific gravities at 25 °C. Tab. 3 provides an overview of the results of the lubricants' viscometric properties. The findings show that viscosity decreases with temperature in all of the samples examined, though the trend varies based on the quantity and kind of solution, with little fluctuation occurring across concentrations because the evaluated additives are not polymeric in nature. This is in line with previous report [43]. If there is not enough viscosity improver in the lubricant, viscosity will fall more quickly when temperature rises, which will damage the lubricating property. However, the combination of EC-CNT and TBHQ demonstrates good compatibility according to FT-IR analysis. This is especially true if the additives are neither homogenous or well compatible with the basic lubricant. With the exception of 1.1 wt.% EC-CNTs + 0.3 wt.% TBHQ, which demonstrates fast drop, the newly formulated SFO + EC-CNTs + TBHQ exhibits some level of sluggish decline as temperature rises. In the analysis, the SFO + 0.3 wt.% TBHQ sample had the lowest performance of all the additives tested.

Table 3. Lubricants Viscometric properties.

Sample/parameter	Kinematic viscosity		Viscosity index (VI)
	40 ºC	100 ºC	
SFO only	34.7	13.3	399.5
SFO + 0.3 % TBHQ	35.3	13.9	409.4
SFO + 0.3 % EC-CNTs	36.2	14.7	420.1
SFO + 0.6% EC-CNTs	36.5	16.1	451
SFO + 0.9% EC-CNTs	37.7	18.3	486.7
SFO + 1.1% EC-CNTs	36.8	16.3	452.5
SFO + 0.3% EC-CNTs + 0.3% TBHQ	36.4	17.1	475.4
SFO + 0.6% EC-CNTs + 0.3% TBHQ	36.5	18.5	504.6
SFO + 0.9% EC-CNTs + 0.3% TBHQ	38.3	19.6	506.5
SFO + 1.1% EC-CNTs + 0.3% TBHQ	38.1	16.8	450

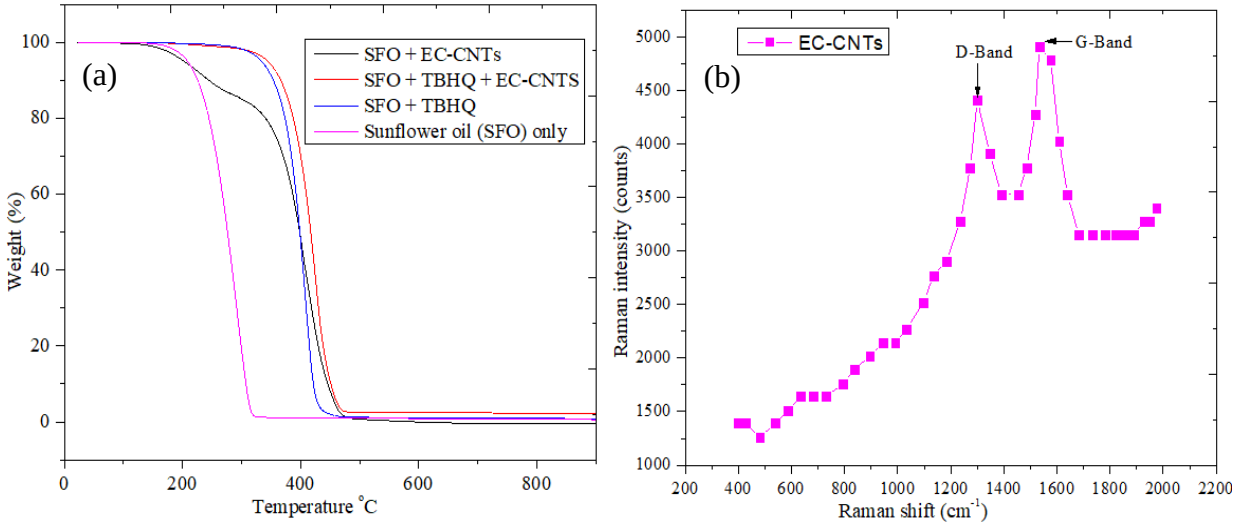

Figure 6. Results of the TGA of SFO, SFO + TBHQ, SFO + EC-CNTs, and SFO + TBHQ + EC-CNTs, showing the weight loss over temperature (a), and Raman spectroscopy of EC-CNTs (b).

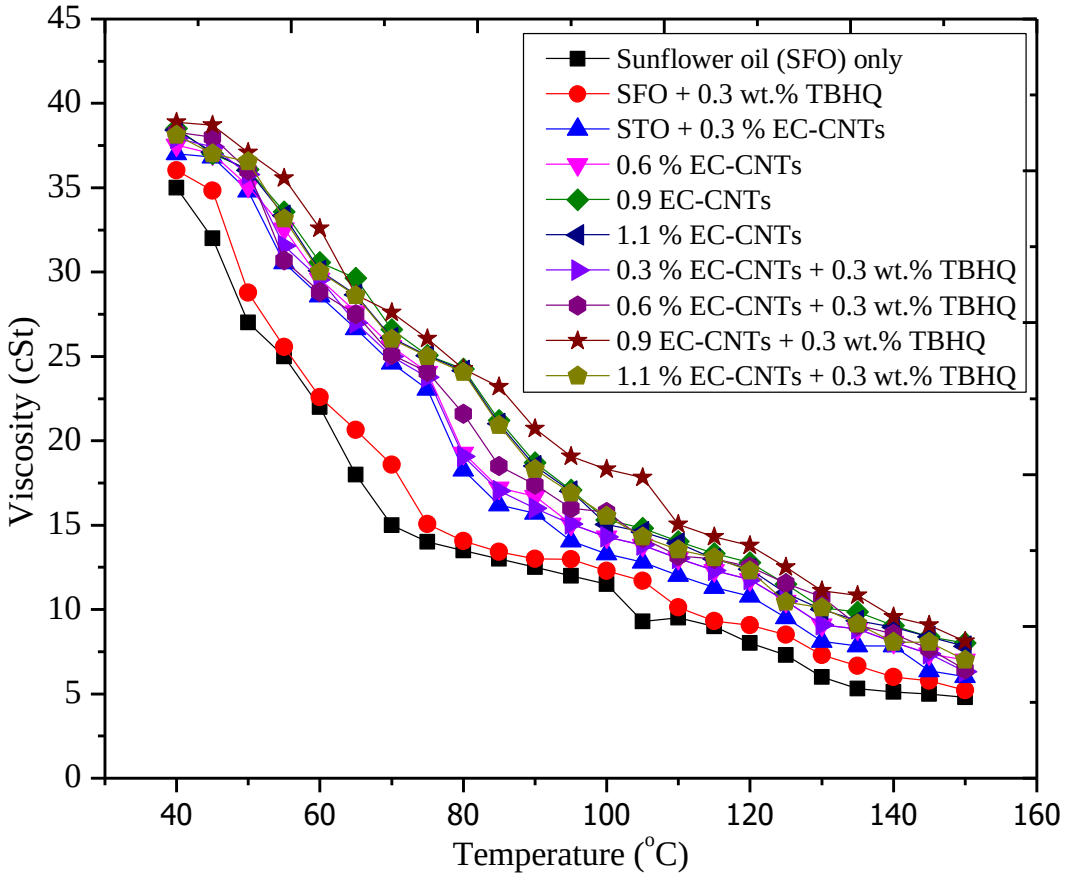

Figure 7. ubricants viscosity against temperatures tested.

The effect of temperature on viscosity is much more pronounced between 40 and 90 oC, but close ranges are seen between 100-150 oC.Due to the heating effect during operation, the additional additives replace the basic lubricant's viscosity even if their operations and degradation resistance are not as robust as those of polymers. At lower temperatures, the viscosity enhancer or polymer chains are compressed, occupy a small molecular volume, and are tightly packed together. But due of the heat impact, the mixed lubricant eventually loses its tribological qualities at high temperatures [43]. When SFO was combined with EC-CNTs and TBHQ, the lubricating oil viscosity index (VI) increases. It can be seen that SFO + TBHQ + EC-CNTs shows the highest VI, followed by 0.9 wt.% EC-CNT, thus used as the best formulation in all the subsequent analysis.

3.2. Coefficient of friction and wear rate under different conditions

As presented in Figure 8, all of the tested lubricants' coefficient of friction and specific wear rate against speed, load and temperature were plotted. In comparison to SFO, SFO + 0.9 % EC-CNTs, and SPO + 0.3 % TBHQ, SFO + 0.9 % EC-CNTs +0.3% TBHQ revealed the lowest coefficient of friction at all speeds, loads and temperatures tested. However, using the additives (EC-CNTs and TBHQ), produces better outcomes than using base SFO. Analyzing SFO, under different speed (Figure 8 (a1)) of 1100, 1300, 1500 and 1700 rpm, the COF was highest with values 0.068, 0.07, 0.074 and 0.078; for load of 60, 80, 100 and 120 as in Figure 8 (b1), yielded 0.064, 0.063, 0.073 and 0.075; while at temperature of 55,75 and 100oC as in Figure 8 (c1), gives 0.065, 0.074 and 0.076, respectively. This shows that loads and temperature give similar results. Following the same sequence, the specific wear rate (Figure 8 (a2)) were 14.8, 15.1, 15.5 and 15.9 10-9 mm3.m-1.N-1 for speed, under load (see Fig. 8 (b2)), gives 14, 13.8, 14 and 14.6 10-9 mm3.m-1.N-1, while for temperature as in Figure 8 (c2) yielded 11.3, 15.3 and 16.4 10-9 mm3.m-1.N-1, respectively.

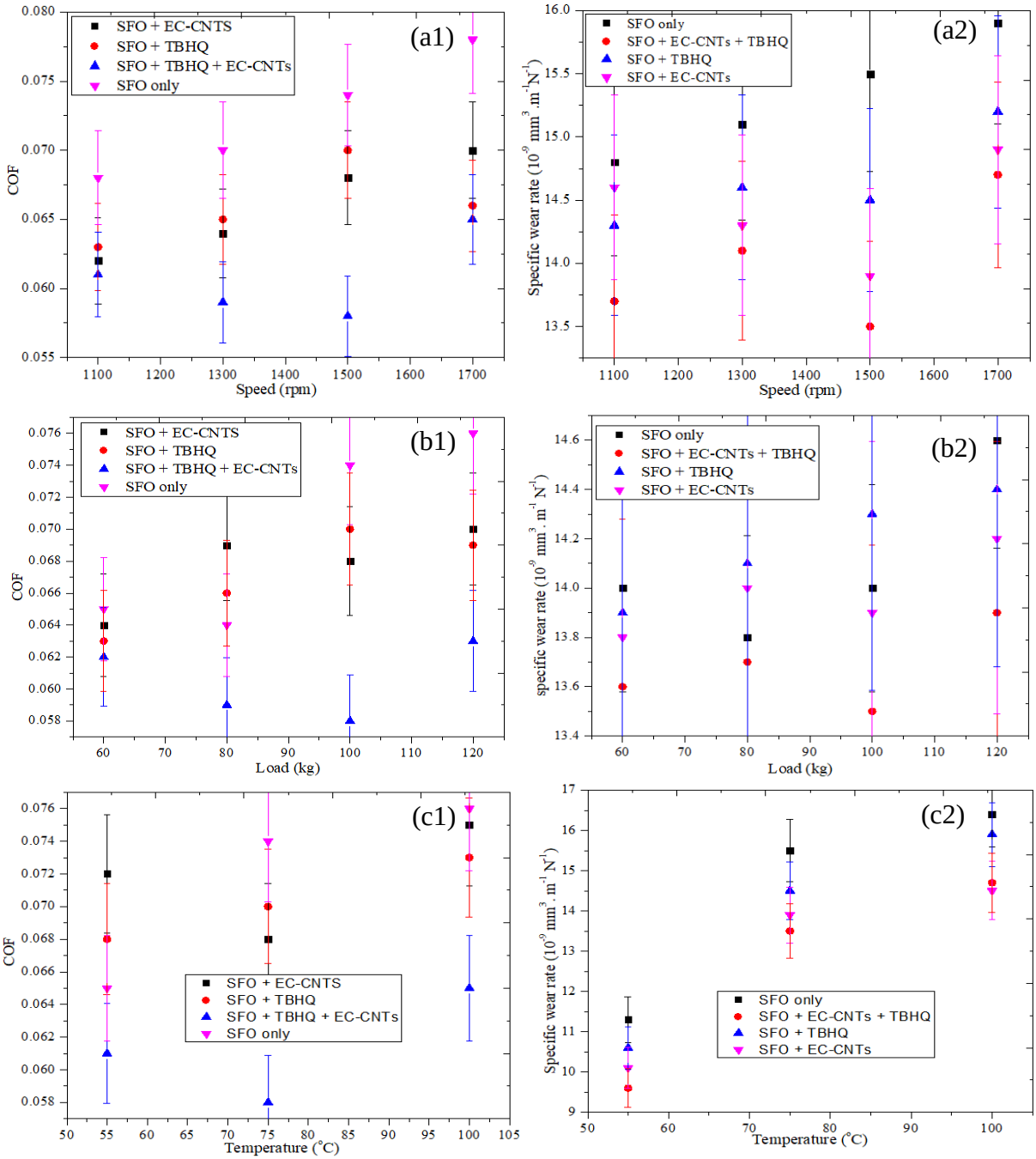

Figure 8. Avg. COF and corresponding specific wear rate (flat disc) for different speed (a1-2) using 100 kg and 75 ºC; load (b1-2) using 1300 rpm and 75 ºC; and temperature (c1-2) using 100 kg and 1300 rpm. (SFO only; SFO + 0.3 wt.% TBHQ; SFO + 0.9wt.% EC-CNTs; SFO + 0.9wt.% EC-CNTs + 0.3 wt.% TBHQ).

In the operation with SFO + 0.9 % EC-CNTs +0.3 % TBHQ, under various speed of 1100, 1300, 1500, 1700 rpm (Figure 8 (a1)), yielded COF of 0.061, 0.059, 0.058 and 0.065; under load of 60, 80, 100 and 120 kg (Fig. 8b1) gives 0.062, 0.059, 0.058 and 0.063; while temperature of 55, 75 and 100 ºC as in Figure 8 (c1), yielded 0.061, 0.058 and 0.065, respectively. When investigating the specific wear rate under the same trend, the various speed as shown in Figure 8 (a2) gives 13.7, 14.1, 13.5 and 14.7 10^{-9} $mm^3.m^{-1}.N^{-1}$; loads (Figure 8 (b2))yielded 13.6, 13.7, 13.5 and 13.9 10^{-9} $mm^3.m^{-1}.N^{-1}$, while temperature (Figure 8 (c2)) gives 9.6, 13.5 and 14.7 10^{-9} $mm^3.m^{-1}.N^{-1}$, respectively. The analysis shows that the best results were found under 1500 rpm, 100 kg, 75 ºC working operations.

The analysis discovered that both high speed, load and temperature, application of additives shows good tribological ability in relative to base SFO. This was attributed to formation of tribo-firm and penetration of NPs between the contacting surface [44] leading to lower COF and wear rate. The observation was supported by the results from the FT-IR analysis and particle size analysis. Furthermore, under different temperatures, the graph shows a similar trend showing that increase in temperature lead in corresponding increase on wear (Figure 8 (c2)). This is due to much generation of friction causing lubricant degradation. Again, the excellent performance recorded from nano-lubricant was due to improved film formation between sliding surfaces and the generation of

frictional energy [25], which improved the lubricant's tribo-chemistry[43][44]. Also, the asperities' carrying forces have been lessened by the long chain of polar fatty acid molecules that firmly connected to the interacting surfaces [44]. However, due to TBHQ's capacity for resisting oxidation during the process, SFO + TBHQ produced superior results at higher speeds than SFO + EC-CNTs. The solution supports the load with a decreased coefficient of friction owing to its outstanding thermo-oxidation properties.

Figure 9 presents the selected disk area wear roughness after operations in terms of surface roughness (Ra), root mean square (Rq) and mean roughness depth (Rz) of disk when lubricated with SFO, SFO + EC-CNTs, SFO + EC-CNTS + TBHQ under best working operation (1500 rpm, 75ºC and 100 kg) corresponding to the results analysis in Figure 6 (a). As shown in Figure 9 (a1-d1), addition of additives indicates reduction on the wears on the lubricated surfaces. The wear nature or healing indicator demonstrating the mechanism and performance of the various lubricants as presented in Figure 9 (a2-d2).As seen in Figures 9(a1 and a2), there was a decrease in surface wear, which revealed crushing and the deposition of nano-additives in the worn areas, causing the surfaces to undergo healing. The results demonstrated synergistic effect when blended the two additives as in Fig. 9 (a1-a2), however, revealed that EC-CNTs (Fig. 9 (b1-2)) gives better surface protection than TBHQ (Figure 9 (c1-2)). The base SFO shows the worst result due to absence of additive, thus expose the balls to direct contact leading to higher values (Fig. 9 (d1-2). The outcome on the surfaces tested indicated that addition of TBHQ + EC-CNTs nanoparticle into the oil can result in less roughness and formation of tribo-film which performs healing on the sliding contact. However, after the friction test with SFO and SFO + TBHQ nanoparticle, roughness of wear scar slightly changes but an increase in roughness related to SFO + EC-CNTs and SFO + EC-CNTs +TBHQ. The observation was due to the anti-wear property of EC-CNTs.

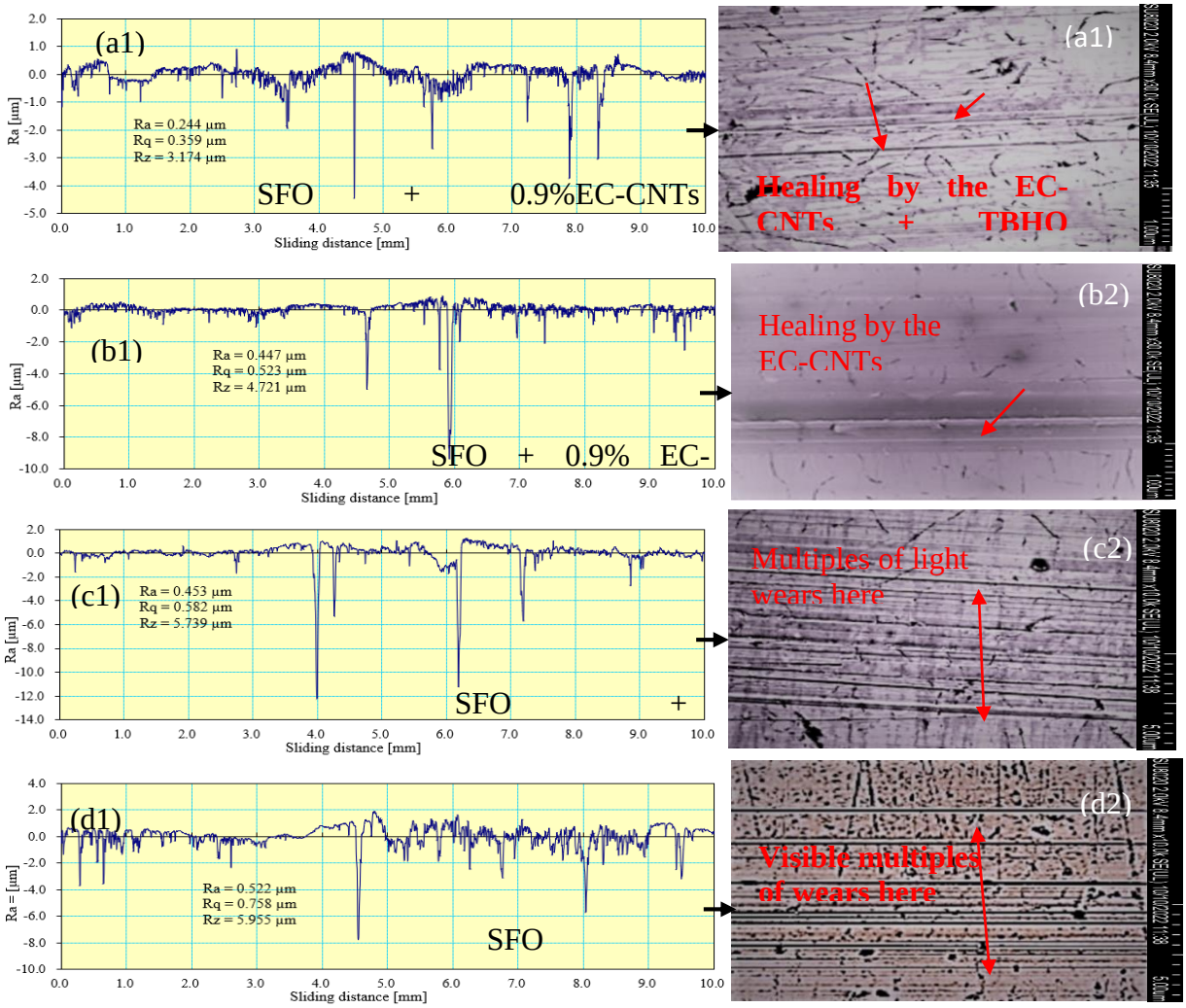

Figure 9. Roughness of wear scar (Ra, Rq, Rz) on the disk lubricated with SFO, SFO + EC-CNTs, SFO + EC-CNTS + TBHQ under speed of 1500 rpm, tempt. 75ºC and 100 kg load.

The analysis of COF and wear scar diameter was further conducted using higher working operation as presented in Figure 10. The wear investigation was carried out by using high resolution microscope equipped with I-Lite Solution software. The result revealed that the average values generated were higher than the outcome under smaller running speed as in Figure 8 (a, b and c). As in Fig 10 (a), the average COF for base SFO was 0.2779, representing the highest COF among all the samples tested, but very close to SFO + EC-CNTs. Under SFO + EC-CNTs, SFO + TBHQ, and SFO + EC-CNTs + TBHQ, COF reduction was 5.9%, 50.5% and 76.8%, respectively against base SFO. The excellent performance from the two additives when used was due to the compatibility among them leading to synergistic effect. Similar result was observed on the analysis conducted using organic anti-wear and ZDDP additive [45].

Evaluating the wear effect from the use of the various samples as presented in Figure 10 (b) using high resolution FESEM machine. The samples exhibited a similar trend, however, demonstrated higher results compared to the smaller working parameters (see Figure 8). The results show that the included additive enhances the tribological performance of SFO. The average WSD under base SFO yielded the highest values in all the load tested. For 60, 80, 100and120 kg load, under base SFO, the average WSD were 0.49, 0.52, 0.5 and 0.57 mm, thus resulted in WSD reduction with SFO + EC-CNTs + TBHQ by 32.7%, 16.7%, 34% and 31.6%, respectively. The wear reduction with EC-CNTs performed better than the use of TBHQ, due to the anti-wear strength of EC-CNTs. Finally, the performance of the nano-lubricant was due to the tribo-film generated and the rolling of the nano particles, which protect the direct contact between the sliding bodies leading to low wear formation.

3.3. Evaluation of average wear scar diameter of the tested sample

Figure 11 illustrated the trend of wear scar diameter against higher speed 2500 rpm using load of 100kg and temperature of 75oC. The result revealed that analysis on speed and load gives similar trends when compared to temperature graphs. The outcome from the entire testing shows that inclusion of additives significantly lowers the wear on the sliding contact except with TBHQ under speed of 1100 and 1500 rpm, when compared to all the tested lubricants. It was also clearly observed that wear scar diameter is having an increasing trend mostly proportionally to the speed, load and temperature increasing for all tested lubricant.

However, under the speed of 1500rpm, SFO + TBHQ + EC-CNTs show significant decrease on the WSD, while at load of 100 kg, SFO + TBHQ + EC-CNTs and SFO + EC-CNTs indicated decrease on WSD against others lubricant graph trend. The rising speed of the sliding motion itself was the cause of the increasing WSD. The fatty acid chain first formed a soap coating on the contacted surfaces during boundary lubrication, which led to fewer asperities contact but not in excess frictional forces.

This motion caused more asperities due to direct contact among the tribo-pairs leading to the removal of material from the contact

surfaces. According to Karmakar et al., [7] during the chemical reaction, the metal surfaces absorb the ester ends of the fatty acid chains, which causes a thin layer of mono film to escape from the metal surfaces. Due to these reactions, the metal surface became weak and was easily worn away by constant sliding. The operating conditions, including temperature, loads, speed, and viscosity, had a significant impact on the durability of these thin layer mono films [48]. The wear rate and condition of the wear surfaces were accelerated by the lubricant's contamination of the hard metal debris that was being removed from the weakened metal surfaces during the sliding motion [49].

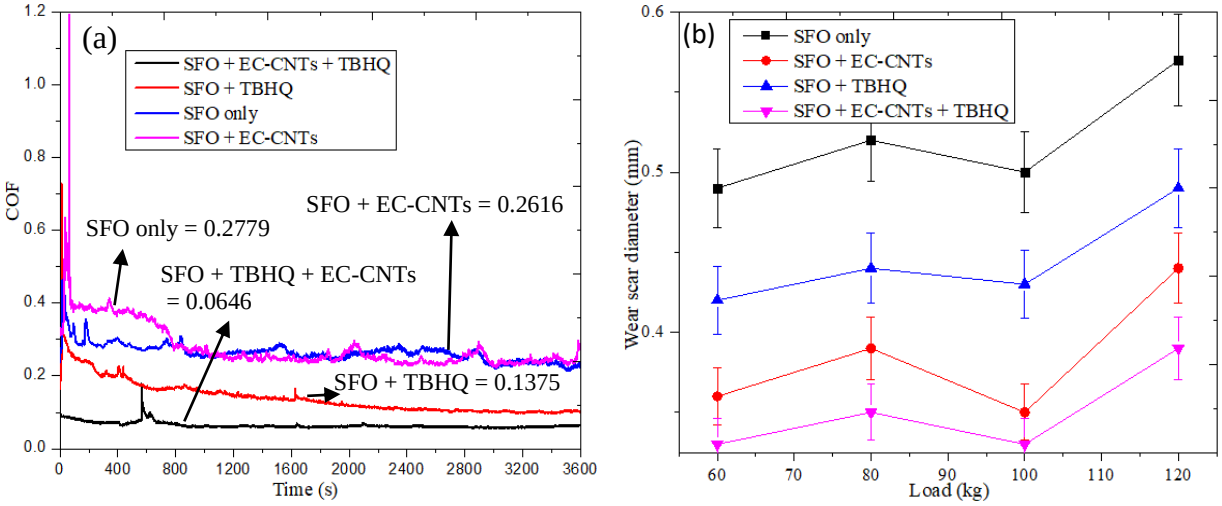

Figure 10. Average COF under speed of 2500 rpm, load of 100 kg, temperature 75 ºC (a) and average WSD under different loads, speed of 2500 rpm, tempt. 75 ºC for the various lubricants.

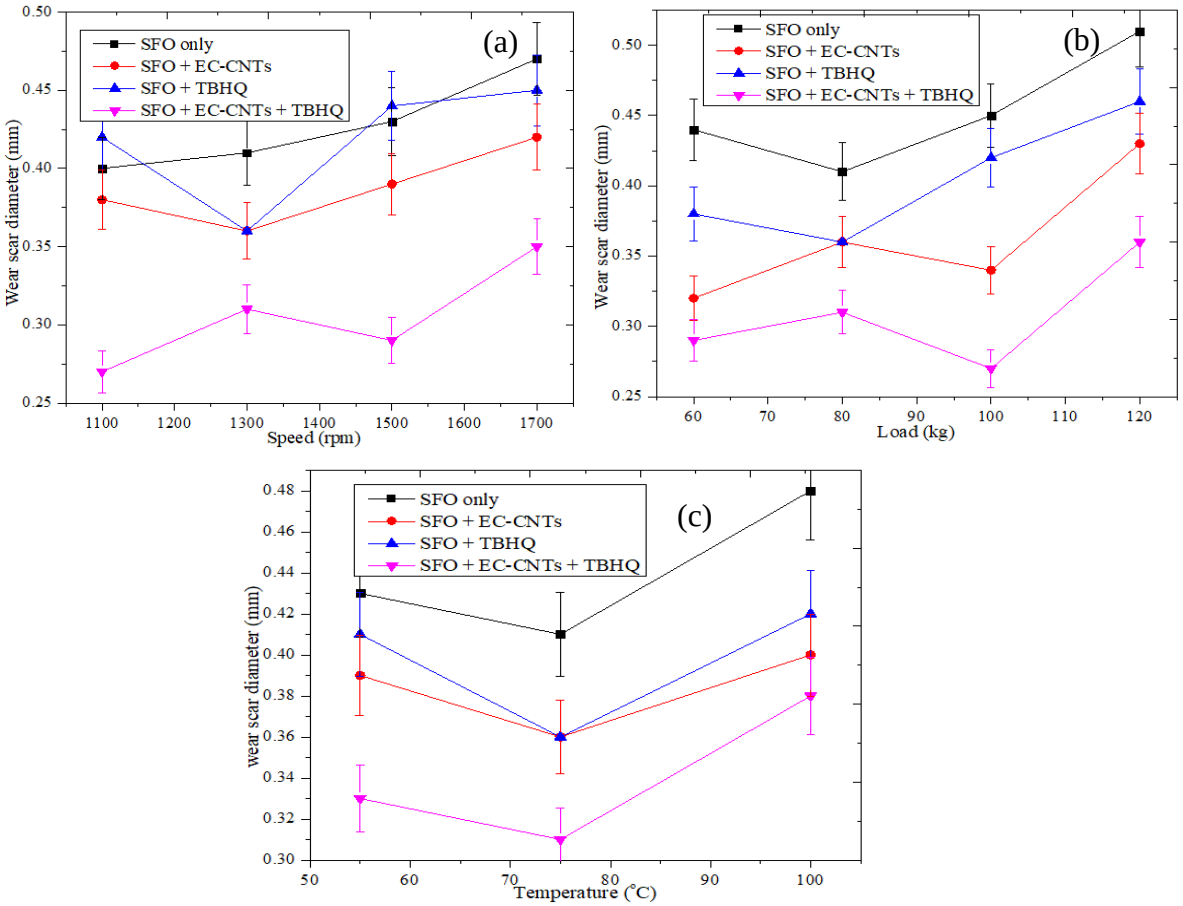

Figure 11. Average WSD for different speeds (a) using 100 kg and 75 ºC; loads (b) using 75 ºC and 1500 rpm; and temperatures (c) using 100 kg and 1500 rpm for the various lubricants.

3.4. Wear surface morphology analysis

The worn surface of the ball after 1hr. operation of bench test is shown in Figure 12 using high resolution SEM incorporated with EDX. After the test, the presence of groves parallel to wear direction is observed in all the lubricated surfaces. As demonstrated in Figure 12, operation using base SFO shows abrasive wears with serious crakes and more metals removed from the surface indicating excessive friction and direct contact operation, however, the observations were similar to the lubrication with SFO + TBHQ, but reduction on the wear diameter. The investigation with SFO + EC-CNTs provided significant reduction on the wear diameter and smoother surface compared base SFO, while nano-lubricant (SFO+TBHQ + EC-CNTs) displayed smoothest surface among all the tested surfaces. The reduction on the grooves was due to the deposition of the nanoparticles at the contact, thus minimized the contact and transferred the sliding motion into rolling motion. This can be concluded that the used additives enhance the properties of the lubricant based on the levels of analysis conducted. On the EDX analysis on the various lubricated surfaces, sample of sunflower alone displayed few elements like Fe and carbon indicating lack of tribo-film formation as presented in Figure 12 (a1), while other surfaces demonstrated formation of film due to additional elements found.

Under sunflower blended TBHQ, additional element was found with higher carbon indication presence of aromatic organic compound as seen in Figure 12 (b1), the surface lubricated with EC-CNT, produces many elements apart from Fe, O and C as illustrated in Figure 12 (c1). Elements like; Al, Si, Mg, Mn, K and Ca which correlates with the results of EDX analysis of EC-CNTs as in Table 2. The detection of those elements was as a result of good tribo-chemistry on the contacted surfaces. During the analysis of surface lubricated with sunflower blended TBHQ and EC-CNT as shown in Figure 12 (d1), some elements were found but lesser to that discovered under EDX analysis of blended EC-CNT. The production of the tribo-film indicated surface separation during the sliding test which could lead to machine elements protections unlike the outcome under application of sunflower alone.

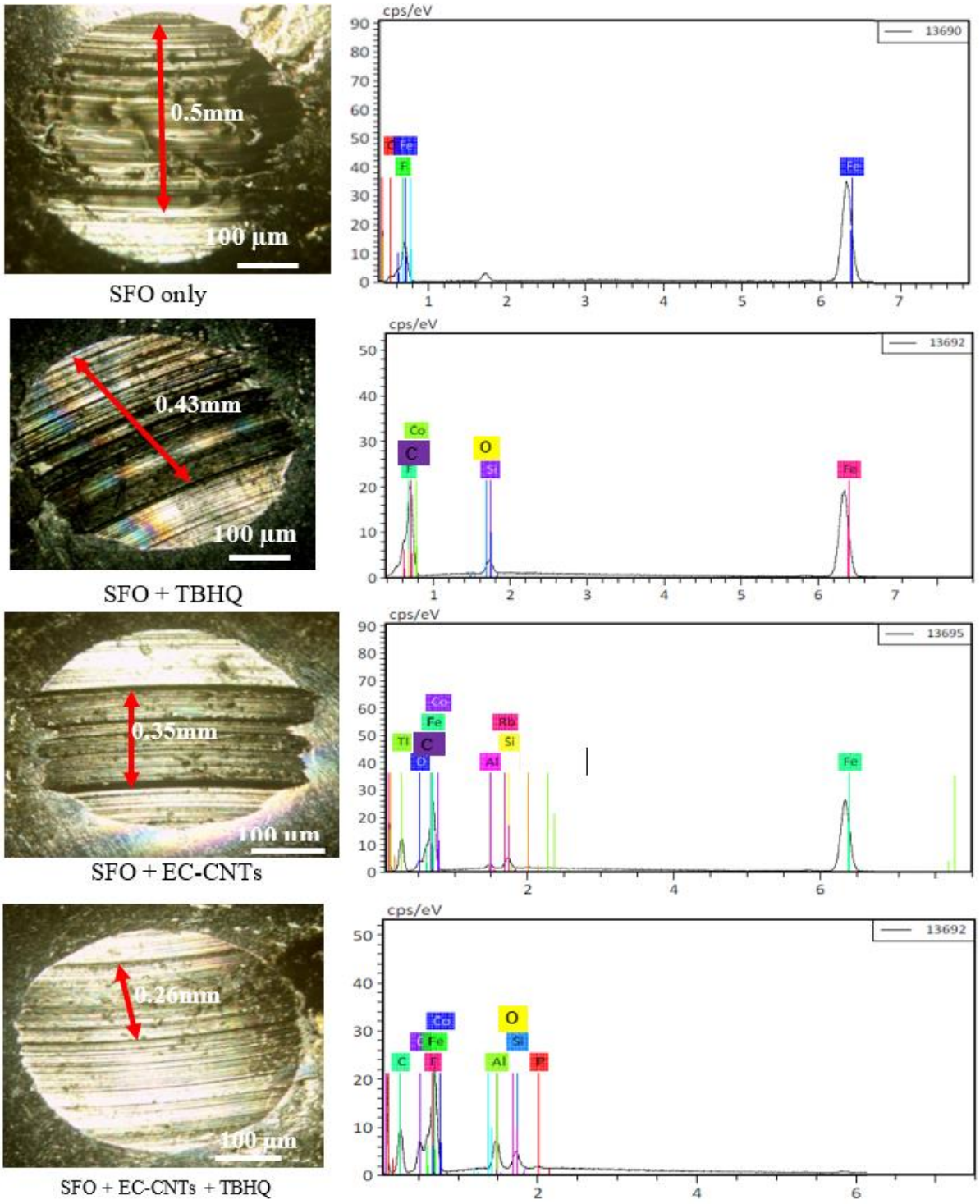

Figure 12. SEM images of the ball lubricated surfaces and the EDX analysis after the operation (2500 rpm, 100 kg, 75 ºC).

3.5. Operating mechanism of SFO + EC-CNTs + TBHQ nano-lubricant

Analyzing the tribological enhancement and synergistic performance from the lubricant. It was observed that due to the penetration at the contact area and the development of tribo-films between the mating surfaces, SFO-nano-lubricants have superior tribological properties compared to their base-oils. The effect of suitable nanoscale needed for lubricant formulation and the related deformation of nanoparticles were reported by Liu et al., and Joly-Pottuz et al., [50][51]. Also, the little concentration used thereby medicates the agglomeration effect which normally causes lubricant starvation within the contact regime. The crushing of NPs has already been established by previous analysis [27] for the formation of film which the study observed. This submission was confirmed due to the existence of nanoparticle elements EC-CNTs particles during the EDX analysis according to Opia et al., [47]. As clearly seen on the wear images in Figure 12, the cracks and serious abrasive wears under base lubrication were not seen much with EC-CNTs and EC-CNTs + TBHQ, thus indicated protective or anti-wear strength of the formulations.

4. Conclusion

In this study, sunflower based bio-lubricant tribological performance was tested under inclusion of anti-wear EC-CNTs and antioxidant of TBHQ. The synergistic behavior under application of the two additive was conducted. The findings indicated that bio-lubricant has the ability to partially replace commercial lubricant, which will reduce reliance on mineral lubricant and lessen the detrimental environmental impact. Again, blending the nano-additives yielded excellent tribological enhancement under all the conditions tested. However, during the use of SFO + EC-CNTs + TBHQ at higher speed of 2500 rpm yielded COF reduction by 76.8% compared to the base SFO reference used. Also shows good reduction on the grooves, crakes and pits which were found on SFO lubricated surface. Finally, application of this nano lubricant will improve machine performance and prolong the lifetime of the machine elements.

Acknowledgments

The authors acknowledge the efforts of the research members of the Green Tribology and Engine Performance Research Group (G-TriboE), UniversitiTeknikal Malaysia Melaka.

References

[1] B. Zareh-Desari and B. Davoodi, "Assessing the lubrication performance of vegetable oil-based nano-lubricants for environmentally conscious metal forming processes," *Journal of Cleaner Production*, vol. 135, pp. 1198–1209, 2016, doi: 10.1016/j.jclepro.2016.07.040.

[2] V. W. Wong and S. C. Tung, "Overview of automotive engine friction and reduction trends–Effects of surface, material, and lubricant-additive technologies," *Friction*, vol. 4, no. 1, pp. 1–17, 2016, doi: 10.1007/s40544-016-0107-9.

[3] P. Zulhanafi and S. Syahrullail, "The tribological performances of Super Olein as fluid lubricant using four-ball tribotester," *Tribology International*, vol. 130. pp. 85–93, 2019. doi: 10.1016/j.triboint.2018.09.013.

[4] J. Shu, K. Harris, B. Munavirov, R. Westbroek, J. Leckner, and S. Glavatskih, "Tribology of polypropylene and Li-complex greases with ZDDP and MoDTC additives," *Tribology International*, vol. 118, no. August 2017, pp. 189–195, 2018, doi: 10.1016/j.triboint.2017.09.028.

[5] C. J. Reeves, A. Siddaiah, and P. L. Menezes, "A Review on the Science and Technology of Natural and Synthetic Biolubricants," *Journal of Bio- and Tribo-Corrosion*, vol. 3, no. 1. 2017. doi: 10.1007/s40735-016-0069-5.

[6] M. K. A. Ali and H. Xianjun, "Improving the tribological behavior of internal combustion engines via the addition of nanoparticles to engine oils," *Nanotechnology Reviews*, vol. 4, no. 4, pp. 347–358, 2015, doi: 10.1515/ntrev-2015-0031.

[7] G. Karmakar, P. Ghosh, and B. K. Sharma, "Chemically modifying velubricantsgetable oils to prepare green," *Lubricants*, vol. 5, no. 4, pp. 1–17, 2017, doi: 10.3390/lubricants5040044.

[8] Abdollah et al., "Experimental analysis of tribological performance of palm oil blended with hexagonal boron nitride nanoparticles as an environment-friendly lubricant," *Advances in Marine Structures*, vol. 106, no. 3, pp. 4183–4191, 2020, doi: 10.1201/b10771-6.

[9] A. C. Opia, M. K. B. A. Hamid, S. Syahrullail, A. B. A. Rahim, and C. A. N. Johnson, "Biomass as a potential source of sustainable fuel, chemical and tribological materials – Overview," *Materials Today: Proceedings*, Apr. 2020, doi: 10.1016/j.matpr.2020.04.045.

[10] Zuan A. and Syahrullail S, "Bio-based Lubricants from Modification of RBD Palm Kernel Oil by TransEsterification," *Journal of Mechanical Engineering*, vol. 4, no. 2, pp. 199–211, 2017.

[11] R. Shah, M. Woydt, and S. Zhang, "The Economic and Environmental Significance of Sustainable Lubricants," *Lubricants*, vol. 3, pp. 1–11, 2021.

[12] D. I. Ahmed, S. Kasolang, R. S. Dwyer-Joyce, K. I. Sainan, and N. R. N. Roselina, "Formulation and physico-chemical characteristics of biolubricant," *Jurnal Tribologi*, vol. 3. pp. 1–10, 2014. [Online]. Available: http://jurnaltribologi.mytribos.org/v3/v3_1.html

[13] B. Bongfa, S. Syahrullail, M. K. Abdul Hamid, and P. M. Samin, "Suitable additives for vegetable oil-based automotive shock absorber fluids: an overview," *Lubrication Science*, vol. 28, no. 6, pp. 381–404, 2016, doi: 10.1002/ls.1337.

[14] H. M. Mobarak, "Non-Edible Oil as a Source of Bio-Lubricant for Industrial Applications : A Review," *International Journal of Engineering Science and Innovative Technology*, vol. 2, no. 1, pp. 299–305, 2013.

[15] M. E. Soltani, K. Shams, S. Akbarzadeh, and A. Ruggiero, "A Comparative Investigation on the Tribological Performance and Physicochemical Properties of Biolubricants of Various Sources, a Petroleum-Based Lubricant, and Blends of the Petroleum-Based Lubricant and Crambe Oil," *Tribology Transactions*, vol. 63, no. 6. pp. 1121–1134, 2020. doi: 10.1080/10402004.2020.1795331.

[16] L. A. Quinchia, M. A. Delgado, C. Valencia, J. M. Franco, and C. Gallegos, "Viscosity modification of different vegetable oils with EVA copolymer for lubricant applications," *Industrial Crops and Products*, vol. 32, no. 3, pp. 607–612, 2010, doi: 10.1016/j.indcrop.2010.07.011.

[17] V. Cortes, K. Sanchez, R. Gonzalez, M. Alcoutlabi, and J. A. Ortega, "The performance of SiO2 and TiO2 nanoparticles as lubricant additives in sunflower oil," *Lubricants*, vol. 8, no. 1. 2020. doi: 10.3390/lubricants8010010.

[18] A. C. Opia, M. F. Bin Abdollah, C. Johnson, SamionSyahrullail, and F. B. M. Zawawi, "Lubricity Performance Evaluation of Organic Polymer as Additives Invegetable Oil Understeel Materials," *Jordan Journal of Mechanical and Industrial Engineering*, vol. 17, no. 3, pp. 385–391, 2023, doi: 10.59038/jjmie/170307.

[19] A. Bahari, "Investigation into Tribological Performance of Vegetable Oils as Biolubricants at Severe Contact Conditions: Department Of Mechanical Engineering, University of Sheffield.," 2017.

[20] G. Gorla, S. M. Kour, K. V. Padmaja, M. S. L. Karuna, and R. B. N. Prasad, "Preparation and properties of lubricant base stocks from epoxidized karanja oil and its alkyl esters," *Industrial and Engineering Chemistry Research*, vol. 52, no. 47, pp. 16598–16605, 2013, doi: 10.1021/ie4024325.

[21] J. McNutt and Q. S. He, "Development of biolubricants from vegetable oils via chemical modification," *Journal of Industrial and Engineering Chemistry*, vol. 36, pp. 1–12, 2016, doi: 10.1016/j.jiec.2016.02.008.

[22] A. S. Kumar, D. Maheswar, and K. V. K. Reddy, "Comparision of Diesel Engine Performance and Emissions from Neat and Transesterified Cotton Seed Oil," *Jordan Journal of Mechanical and Industrial Engineering*, vol. 3, no. 3, pp. 190–197, 2009.

[23] Liu et al., "Thermal losses of tertiary butylhydroquinone (TBHQ) and its effect on the qualities of palm oil," *Journal of Oleo Science*, vol. 65, no. 9. pp. 739–748, 2016. doi: 10.5650/jos.ess16041.

[24] A. I. Ali *et al.*, "Tribological Performance Evaluation of Vegetable Lubricant Incorporated Ethylene Vinyl Acetate (EVA) and Tertiary-Butyl-Hydroquinone (TBHQ) Nanoparticles," *Tribology Online*, vol. 18, no. 4, pp. 103–114, 2023, doi: 10.2474/trol.18.103.

[25] M. K. A. Ali, H. Xianjun, A. Elagouz, F. A. Essa, and M. A. A. Abdelkareem, "Minimizing of the boundary friction coefficient in automotive engines using Al2O3 and TiO2 nanoparticles," *Journal of Nanoparticle Research*, vol. 18, no. 12, pp. 1–38, 2016, doi: 10.1007/s11051-016-3679-4.

[26] A. N. Afifah, S. Syahrullail, M. Amirrul Amin, and H. M. Faizal, "Mechanical properties of palm kernel oil-copper oxide nanolubricant," *Jurnal Teknologi*, vol. 79, no. 7–4, pp. 61–66, 2017, doi: 10.11113/jt.v79.12266.

[27] A. C. Opia *et al.*, "Tribological behavior of organic formulated anti-wear additive under high frequency reciprocating rig and unidirectional orientations: Particles transport behavior and film formation mechanism," *Tribology International*, vol. 167, pp. 1–34, 2022, doi: 10.1016/j.triboint.2021.107415.

[28] H. Xie, B. Jiang, J. He, X. Xia, and F. Pan, "Lubrication performance of MoS2 and SiO2 nanoparticles as lubricant additives in magnesium alloy-steel contacts," *Tribology International*, vol. 93, pp. 63–70, 2016, doi: 10.1016/j.triboint.2015.08.009.

[29] E. O. L. Ettefaghi, H. Ahmadi, A. Rashidi, and S. S. Mohtasebi, "Investigation of the anti-wear properties of nano additives on sliding bearings of internal combustion engines," *International Journal of Precision Engineering and Manufacturing*, vol. 14, no. 5, pp. 805–809, 2013, doi: 10.1007/s12541-013-0105-z.

[30] M. A. Amrani *et al*., "A Lubricating Oil-Based Maintenance for Diesel Engines at the End-user: An Effective Predictive Approach," *Jordan Journal of Mechanical and Industrial Engineering*, vol. 16, no. 5, pp. 689–700, 2022.

[31] N. Kapilan, "Impact of carbon nano tubes on the performance and emissions of a diesel engine fuelled with pongamia oil biodiesel," *Jordan Journal of Mechanical and Industrial Engineering*, vol. 15, no. 3, pp. 283–290, 2021.

[32] G. C. Cristea, C. Dima, C. Georgescu, D. Dima, L. Deleanu, and L. C. Solea, "Evaluating lubrication capability of soybean oil with nano carbon additive," *Tribology in Industry*, vol. 40, no. 1, pp. 66–72, 2018, doi: 10.24874/ti.2018.40.01.05.

[33] A. Aravind, M. L. Joy, and K. P. Nair, "Lubricant properties of biodegradable rubber tree seed (Hevea brasiliensis Muell. Arg) oil," *Industrial Crops and Products*, vol. 74. pp. 14–19, 2015. doi: 10.1016/j.indcrop.2015.04.014.

[34] N. K. Attia, S. A. El-Mekkawi, O. A. Elardy, and E. A. Abdelkader, "Chemical and rheological assessment of produced biolubricants from different vegetable oils," *Fuel*, vol. 271. 2020. doi: 10.1016/j.fuel.2020.117578.

[35] T. V. Rao, G. P. Rao, and K. H. Chandra, "Experimental Investigation of Pongamia, Jatropha and Neem Methyl Esters as Biodiesel on C.I. Engine," *Jordan Journal of Mechanical and Industrial Engineering*, vol. 2, no. 2, pp. 117–122, 2008.

[36] A. V. Kolhe, R. E. Shelke, and S. S. Khandare, "Performance and combustion characteristics of a DI diesel engine fueled with jatropha methyl esters and its blends," *Jordan Journal of Mechanical and Industrial Engineering*, vol. 8, no. 1, pp. 7–12, 2014.

[37] C. P. Koshy, P. K. Rajendrakumar, and M. V. Thottackkad, "Evaluation of the tribological and thermo-physical properties of coconut oil added with MoS2 nanoparticles at elevated temperatures," *Wear*, vol. 330–331, pp. 288–308, 2015, doi: 10.1016/j.wear.2014.12.044.

[38] J. B. He, H. Shi, Y. Wang, and X. L. Gao, "Synthesis, characterization, and performance evaluation of sulfur-containing diphenylamines based on intramolecular synergism," *Molecules*, vol. 23, no. 2, 2018, doi: 10.3390/molecules23020401.

[39] M. M. H. Bastwros, A. M. K. Esawi, and A. Wifi, "Friction and wear behavior of Al-CNT composites," *Wear*, vol. 307, no. 1–2, pp. 164–173, 2013, doi: 10.1016/j.wear.2013.08.021.

[40] P. Kumar Gupta *et al.*, "An Update on Overview of Cellulose, Its Structure and Applications," *Cellulose [Working Title]*, pp. 1–22, 2019, doi: 10.5772/intechopen.84727.

[41] T. Zhang, M. Xiao, Z. Zhang, W. Li, and J. Bai, "Production and Properties of Carbon Nanotube/Cellulose Composite Paper," pp. 1–12, 2021.

[42] S. Nasir, M. Z. Hussein, Z. Zainal, and N. A. Yusof, "Carbon-based nanomaterials/allotropes: A glimpse of their synthesis, properties and some applications," *Materials*, vol. 11, no. 2, pp. 1–24, 2018, doi: 10.3390/ma11020295.

[43] S. I. Shara, E. A. Eissa, and J. S. Basta, "Polymers additive for improving the flow properties of lubricating oil," *Egyptian Journal of Petroleum*, vol. 27, no. 4, pp. 795–799, 2018, doi: 10.1016/j.ejpe.2017.12.001.

[44] S. M. Alves, B. S. Barros, M. F. Trajano, K. S. B. Ribeiro, and E. Moura, "Tribological behavior of vegetable oil-based lubricants with nanoparticles of oxides in boundary lubrication conditions," *Tribology International*, vol. 65, pp. 28–36, 2013, doi: 10.1016/j.triboint.2013.03.027.

[45] M. K. A. Ali, H. Xianjun, L. Mai, C. Qingping, R. F. Turkson, and C. Bicheng, "Improving the tribological characteristics of piston ring assembly in automotive engines using Al2O3 and TiO2 nanomaterials as nano-lubricant additives," *Tribology International*, vol. 103, pp. 540–554, 2016, doi: 10.1016/j.triboint.2016.08.011.

[46] M. N. Abijith, A. R. Nair, M. Aadharsh, R. V. Vignesh, R. Padmanaban, and M. Arivarasu, "Investigations on the mechanical, wear and corrosion properties of cold metal transfer welded and friction stir welded aluminium alloy AA2219," *Jordan Journal of Mechanical and Industrial Engineering*, vol. 12, no. 4, pp. 281–292, 2018.

[47] Opia et al., "Tribological Behavior of Organic Anti-Wear and Friction Reducing Additive of ZDDP under Sliding Condition : Synergism and Antagonism Effect," *Evergreen*, vol. 09, no. 02, 2022.

[48] M. Shahabuddin, H. H. Masjuki, and M. A. Kalam, "Experimental investigation into tribological characteristics of biolubricant formulated from Jatropha oil," *Procedia Engineering*, vol. 56. pp. 597–606, 2013. doi: 10.1016/j.proeng.2013.03.165.

[49] M. A. Kalam, H. H. Masjuki, M. Varman, and A. M. Liaquat, "Friction and wear characteristics of waste vegetable oil contaminated lubricants," *International Journal of Mechanical and Materials Engineering*, vol. 6, no. 3, pp. 431–436, 2011.

[50] G. Liu, X. Li, B. Qin, D. Xing, Y. Guo, and R. Fan, "Investigation of the mending effect and mechanism of copper nano-particles on a tribologically stressed surface," *Tribology Letters*, vol. 17, no. 4, pp. 961–966, 2004, doi: 10.1007/s11249-004-8109-6.

[51] L. Joly-Pottuz, B. Vacher, N. Ohmae, J. M. Martin, and T. Epicier, "Anti-wear and friction reducing mechanisms of carbon nano-onions as lubricant additives," *Tribology Letters*, vol. 30, no. 1, pp. 69–80, 2008, doi: 10.1007/s11249-008-9316-3.